EFFECT OF VARIATIONS IN THE ATMOSPHERIC OPTICAL PROPERTIES ON THE ACCURACY OF LOWER–TROPOSPHERIC OZONE SOUNDING IN THE UV

V.V. Zuev, A.A. Mitsel', and I.V. Ptashnik

Institute of Atmospheric Optics,
Siberian Branch of the Russian Academy of Sciences, Tomsk
Received May 29, 1992

The effect of water vapour absorption and aerosol and molecular scattering in the UV on the accuracy of reconstructing the ozone profiles from lidar data obtained in the lower troposphere is numerically estimated. Simultaneous measurement of the profiles of the water vapour and aerosol concentrations is shown to be necessary for successful interpretation of lidar ozone data.

INTRODUCTION

Atmospheric ozone has attracted close attention of specialists in the field of laser monitoring of air basin since the 70's.[1–4] A new method known as ozonometry came into being[5,6] which has such advantages as high spatiotemporal resolution and feasibility of measurements on any paths and at any distances. A differential absorption lidar (DIAL) method is most sensitive among laser methods.[7]

The UV is most suitable for ozone sounding for a number of reasons. (1) Strong electron absorption bands (Hartley bands) with an absorption cross section of $1.08 \cdot 10^{-17}$ cm^2 in maximum ($\lambda = 255$ nm) (Ref. 8) and the weaker Huggins 310–340 nm bands lie here. (2) Backscattered signals in the UV exceed essentially the signals in the IR. (3) Reasonably high–power coherent sources of radiation based on excimer lasers are available in the UV. In combination with SRS cells, synchronous sounding pulses at two wavelengths (λ_{on} and λ_{off}) can be obtained. Solid–state lasers with frequency converters are no less promising. (4) High–sensitive photodetectors (photomultipliers) are available for record of the UV radiation. They allow one to detect weak signals from long distances (up to 50 km).

At present the principal results of high–altitude ozone sounding with ground–based lidars have been obtained not only for the stratosphere, in which the maximum of the ozone layer is, but also for the troposphere.[9–27] As reported, ozone sounding is performed by airborne lidars.[16,25] In recent years laser sounding of tropospheric ozone is carried out most actively as part of the EUROTRAC project.[28]

Simultaneously with the O_3 bands, a number of molecules such as SO_2, NO_2, HNO_3, H_2O_2, N_2O_5, HNO_2, H_2CO, and C_7H_8 have their absorption bands in the UV (see Refs. 23, 29, and 30). The UV radiation absorption by these gases leads to the distortion of the O_3 sounding results. Moreover, the wavelengths λ_{on} and λ_{off} should be widely spaced because of strong overlap of the O_3 bands (unresolved structure), so that the nonselective losses of radiation due to molecular inhomogeneities and aerosol particles are different at these wavelengths. This also causes distortion of the results of sounding.

The effect of interfering gases on the accuracy of stratospheric ozone sounding was analyzed in Refs. 5 and 31. In these papers it was concluded that the absorption due to H_2O, SO_2, NO_2. HNO_3, H_2O_2, and N_2O_5 was negligible in comparison with that due to O_3 in the wavelength region 290–320 nm. Contribution of the interference of SO_2 and NO_2 to sounding radiation absorption was analyzed in Ref. 22. We informed about the study of potentials of the DIAL method for tropospheric and stratospheric ozone sounding in Ref. 32. The emphasis was on the errors caused by the measurement noise of lidar returns and uncompensated nonselective losses of radiation power due to molecular inhomogeneities and aerosol particles.

The observation of a new absorption band having its maximum at a wavelength of 270 nm in the near–UV has been reported[33] in recent years. An estimated maximum absorption coefficient was equal to 10^{-6} cm^{-1} (see Ref. 33) for a water vapour concentration of $4 \cdot 10^{17}$ cm^{-3}. An investigation of the long–wave wing of the H_2O absorption band using a tuneable wavelength–doubled dye laser was reported in Ref. 34. The measurements with resolutions of 0.03 and 0.003 nm were made in laboratory conditions. The linear structure was not found.

Absolute measurements of the absorption coefficients in multipass cells with bases of 2 and 110 m were reported in Refs. 35–37. The absorption coefficient at a wavelength of 266 nm (the fourth harmonic of a Nd : YAG laser) was $0.8 \cdot 10^{-6}$ cm^{-1}/Torr (optical path length was equal to 440 m). Presented in Ref. 37 quantitative results span the wavelength region 270–360 nm. The range of variation of the absorption coefficients was 0–$2.8 \cdot 10^{-6}$ cm^{-1}/Torr.

In this paper the effect of the variability of the atmospheric optical properties caused by the variations in gas concentrations (first of all, of water vapour) and aerosol component on the accuracy of lower–tropospheric ozone sounding ($H \le 5$ km) is analyzed using the UV radiation at the following three pairs of wavelengths: (1) 266 and 289 nm (the fourth harmonic of the Nd : YAG laser and the first Stokes component excited in the SRS cell with D_2), (2) 277 and 313 nm (the first and second Stokes components excited by a KrF–laser radiation in the SRS cell with H_2), and (3) 289 and 299 nm (the first Stokes components excited by radiation of the fourth harmonic of the Nd : YAG laser in the SRS cell with D_2 and H_2, respectively).

0235-6880/92/10 675-06 $02.00

INVESTIGATION TECHNIQUE AND RESULTS OF COMPUTER SIMULATION

Let us write down the relation for the ozone concentration $\rho_{O_3}(z)$ derived from lidar returns $U_{on}(z)$ and $U_{off}(z)$

$$\rho_{O_3}(z) = \frac{1}{K_{O_3}(z)\Delta z} \times \left\{ \frac{1}{2} \ln \left[\frac{U_{off}(z + \Delta z) U_{on}(z)}{U_{on}(z + \Delta z) U_{off}(z)} - \alpha_{res} \Delta z \right] \right\}, \quad (1)$$

$$\alpha_{res}(z) = \frac{1}{2\Delta z} \ln \left[\frac{\beta_{off}(z + \Delta z)\beta_{on}(z)}{\beta_{on}(z + \Delta z)\beta_{off}} \right] +$$

$$+ \left[\alpha_{on}(z) - \alpha_{off}(z) \right] + \sum_i \left[\alpha^i_{on}(z) - \alpha^i_{off}(z) \right], \quad (2)$$

$$K_{O_3}(z) = K^{O_3}_{on}(z) - K^{O_3}_{off}(z) . \quad (3)$$

Here $\alpha_{res}(z)$ is the coefficient of residual extinction[32] at the altitude z, Δz is the altitude resolution, and $\beta_{on}(z)$, $\beta_{off}(z)$, $\alpha_{on}(z)$, and $\alpha_{off}(z)$ are the coefficients of backscattering and extinction, respectively, at the altitude z and the wavelengths λ_{on} and λ_{off}, being equal to

$$\beta_{on,off}(z) = \beta^a_{on,off}(z) + \beta^m_{on,off}(z) , \; \alpha_{on,off}(z) = \alpha^a_{on,off}(z) + \alpha^m_{on,off}(z), \quad (4)$$

where the superscripts a and m denote aerosol and molecular scattering and $\alpha^i_{on,off}(z)$ is the absorption coefficient of the ith interfering gas.

The difference of the coefficients $(\alpha_{on} - \alpha_{off})$ determines the uncompensated extinction at two wavelengths due to molecular scattering and aerosol extinction and $\sum_i \alpha^i_{on} - \alpha^i_{off}$ is the uncompensated absorption of interfering gases.

From Eq. (1) it follows that α_{res} introduces the systematic error in measuring the O_3 concentration (systematic bias of the estimate of ρ_{O_3}). The coefficient α_{res} can be represented in the form

$$\alpha_{res} = \alpha^{(a-m)}_{res} + \alpha^g_{res} , \quad (5)$$

where $\alpha^{(a-m)}_{res}$ is the coefficient of residual extinction due to aerosol and molecular scattering and α^g_{res} is the uncompensated absorption due to interfering gases. The optical model of aerosol[38] and the data on molecular scattering[39] with the $3/8\pi$ backscattering phase function can be used in order to estimate $\alpha^{(a-m)}_{res}$. The altitude profiles of the pressure and temperature can be borrowed, for example, from Ref. 40 for calculation of molecular scattering coefficients. Let us present the quantitative data on the coefficient α^g_{res}.

Information about the absorption coefficients $K^i_{on,off}$ of the interfering gases and gas concentration profiles ρ_i or their partial pressures $P_i(z)$ is necessary for calculation of α^g_{res}. According to the preliminary estimates the primary contribution to α^g_{res} in the lower troposphere comes from H_2O, SO_2, and NO_2. The $P_i(z)$ profiles for the investigated O_3 gas and interfering gases H_2O, SO_2, and NO_2 are shown in Fig. 1. The statistically average model profiles of the O_3 and N_2O concentrations are shown by solid lines and their variation corridors within the standard deviation for the mid–latitudes in summer[40] — by dashed lines. The H_2O profile with the inversion at an altitude of 600 m obtained during one of the sounding runs over Tomsk[41] is also shown in Fig. 1*b*. The SO_2 profiles obtained over the industrial zone[42] are given. Above 1 km the SO_2 profile was extrapolated from model data while the NO_2 profile — from data of Ref. 44.

The differential absorption coefficients of ozone and interfering gases were calculated using the absorption coefficients borrowed from the literature (see Table I). The results are shown in Fig. 2. The ranges of possible values of differential absorption coefficients of ozone and water corresponding to the corridors of their concentration (Figs. 1*a* and *b*) are also shown there.

TABLE I. The absorption coefficients K ($atm^{-1}cm^{-1}$).

Serial number	λ (nm)	O_3 (Ref. 45)	H_2O (Ref. 37)	SO_2 (Refs. 30 and 46)	NO_2 (Ref. 47)
1	266 289	245 39	2.0·10–3 1.1·10–3	12.5 26	0.55 2.12
2	277 313	129 1.58	1.5·10–3 6.0·10–4	18.5 6.5	1.23 5.20
3	289 299	39 11	1.1·10–3 7.7·10–4	26 10	2.12 2.88

Figure 2 shows that the primary contribution to α_{res} comes from H_2O. Moreover, the value of α_{H_2O} may essentially exceed that of ozone at altitudes below 2 km. This is most pronounced for the third pair (289 and 299 nm) for which it can reach an order of magnitude.

SO_2 can affect the results of ozone sounding only over the industrial areas in which the near–ground concentration of SO_2 can be several factors of ten larger than the background ($0.3 \cdot 10^{-9}$ atm) (see Fig. 1*c*).[43] This may result in the error in determining the ozone concentration as large as 5–10% for the first and second pairs and as large as 30% and more for the 289 and 299 nm pair.

The effect of NO_2 can be neglected. However, it should be remembered that the NO_2 concentration in the ground layer may be several hundred times larger than the background and hence the value of α_{NO_2} may be comparable to α_{O_3}.

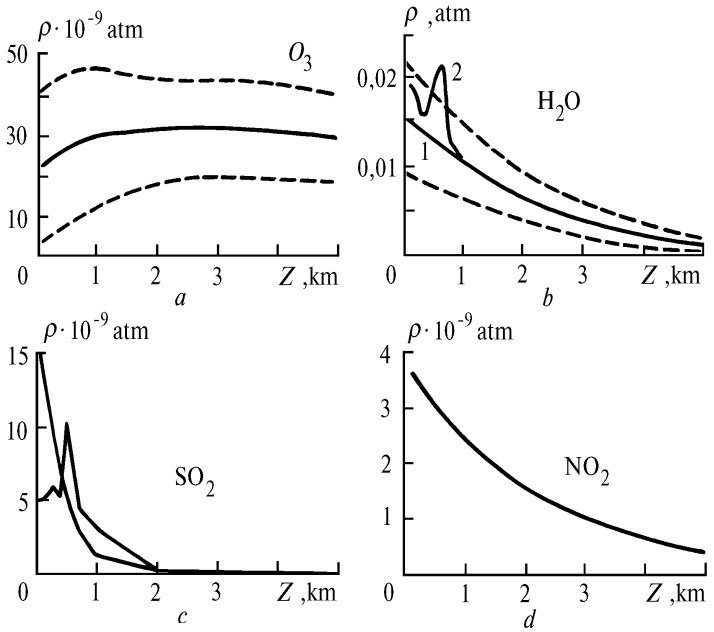

FIG. 1. Partial pressures of the O_3, H_2O, SO_2, *and* NO_2 *gases.*

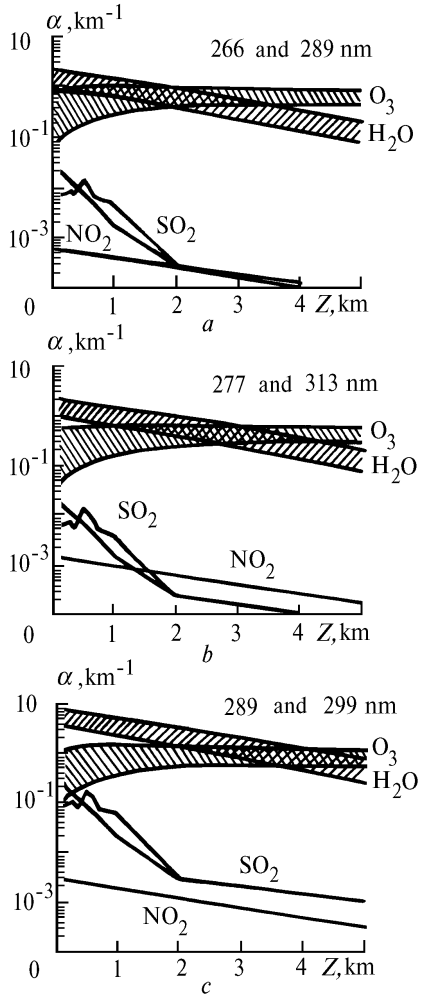

FIG. 2. Differential absorption coefficients of O_3 *and* H_2O, SO_2, *and* NO_2 *interfering gases for the three pairs of wavelengths. The hatched areas show the range of variation of the absorption coefficients of* O_3 *and* H_2O.

Hence the primary contribution to α_{res}^{g} comes from H_2O for all three pairs of wavelengths under consideration. Neglect of this factor may cause highly overestimated ozone concentration derived from lidar returns in the lower troposphere. Thus for the 289 and 299 nm pair this overestimate in some cases may reach an order of magnitude in summer. In winter the distortion of the ozone sounding results caused by neglect of the UV absorption by water vapour is approximately three times smaller.

Therefore, the data on the profiles of concentration, first of all, of water vapour are necessary to eliminate the systematic error in determining ρ_{O_3} from lidar data. If the lidar is placed near industrial areas the information about the concentrations of SO_2 and NO_2 is also needed. Moreover, proper allowance must be made for α_{res}^{a-m} caused by aerosol and molecular scattering.

The coefficients of residual extinction α_{res} can be determined by three ways.

The first way is based on the experimental data on the aerosol coefficients $\beta_{on,off}^{a}$ and $\alpha_{on,off}^{a}$ and concentration profiles of interfering gases ρ^i. To obtain them, the lidar system must be complemented by spectral channels for measuring the aerosol and gaseous components. The coefficients of molecular scattering $\beta_{on,off}^{m}$ and $\alpha_{on,off}^{m}$ are calculated using the model profiles of pressure and temperature. *The second way* of determining the residual extinction coefficient is to calculate it, using the model profiles of β^a, α^a, and ρ^i. *The third way* is combined. It implies that the components, which are of primary importance for the residual extinction, are experimentally determined whereas the rest of the components are calculated from model data.

The first way of determining α_{res} allows one to eliminate practically completely the systematic error in determining ρ_{O_3}. The second way decreases but does not eliminate completely the error of ozone profile sounding caused by possible deviations of real profiles of β^a, α^a, and gas concentrations from the model ones. Let us derive for the last case the relation for the total relative error ε caused by variations of α_{res} and lidar returns.

Let us introduce the following approximations:

$$\alpha^{a}_{off} = g^{a}_{\alpha}\,\alpha^{a}_{on},\ \beta^{a}_{off} = g^{a}_{\beta}\,\beta^{a}_{on},\ \alpha^{m}_{off} = g_{m}\alpha^{m}_{on},\ \beta^{m}_{off} = g_{m}\,\beta^{m}_{on},$$

$$g^{a}_{\alpha} = \left(\frac{\lambda_{on}}{\lambda_{off}}\right)^{q_\alpha},\ g^{a}_{\beta} = \left(\frac{\lambda_{on}}{\lambda_{off}}\right)^{q_\beta},\ g_{m} = \left(\frac{\lambda_{on}}{\lambda_{off}}\right)^{4}.$$

We can than write down ε in the form

$$\varepsilon = \frac{\sigma_q}{\rho_{O_3}} = \frac{1}{K_{O_3}\rho_{O_3}\Delta z}\left\{\frac{1}{4n}\gamma^2 + \sigma^{a}_{\alpha_{res}}(\Delta z)^2\right\}^{1/2}, \qquad (6)$$

$$\gamma^2 = 2\left[\left(\frac{\sigma_{on}}{U_{on}}\right)^2 + \left(\frac{\sigma_{off}}{U_{off}}\right)^2\right], \qquad (7)$$

$$\sigma^{a}_{\alpha_{res}} = \frac{1}{2(\Delta z)^2}\left(\delta^2_{\beta_a} + \delta^2_{\beta_m}\right)\left(\frac{\beta^{a}_{off}\,\beta^{m}_{on} - \beta^{a}_{on}\,\beta^{m}_{off}}{\beta_{on}\,\beta_{off}}\right)^2 +$$

$$+ \frac{1}{2(\Delta z)^2}\,\delta^2_{q_\beta}\left(\frac{\beta^{a}_{off}}{\beta_{off}}\ln g^{a}_{\beta}\right)^2 +$$

$$+ \left[\delta^2_{q_a}\left(\alpha^{a}_{off}\ln g^{a}_{\alpha}\right)^2 + \left(\alpha^{a}_{on} - \alpha^{a}_{off}\right)^2\delta^2_{\alpha_a} +\right.$$

$$\left. + \left(\alpha^{m}_{on} - \alpha^{m}_{off}\right)^2\delta^2_{\alpha_m} + \sum_i\left(\alpha^{i}_{on} - \alpha^{i}_{off}\right)^2\delta^2_{\rho_i}\right]. \qquad (8)$$

Here, n is the number of pulse pairs; γ is the error caused by the error in measuring the signals; δ_{β_a} and δ_{β_m} are the relative errors of determining the Mie and Rayleigh backscattering coefficients; δ_{α_a}, δ_{α_m}, δ^{ρ}_{i}, δ_{q_β}, and δ_{q_α} are the relative errors in determining the extinction coefficients due to aerosol component and molecular scattering, the it interfering gas concentration, and the coefficients describing the spectral behaviour q_β and q_α, respectively. In the derivation of formula (8) the random variables $\alpha(z + \Delta z)$ and $\alpha(z)$ were assumed uncorrelated (here $\alpha(z)$ is taken to mean either β^{a} or q_β). This assumption is used here because of the lack of information about the altitude profiles of correlation coefficients of the above–mentioned quantities. As a consequence formula (8) will estimate the maximum error in determining the residual extinction coefficient.

In the paper we ignore the error in measuring the signals; therefore, the term $\frac{1}{4n}\gamma^2$ in Eq. (6) is omitted.

As mentioned above, the primary contribution to α^{g}_{res} comes from water vapour. In this connection the error caused by the model which accounts for interfering gases will be analyzed only for H_2O. The errors caused by complete neglect of the UV radiation absorption by water vapour in lidar data processing are shown by dashed lines in Fig. 3. It can be seen that the error within the 100–500 m altitude range amounts up to 200–300% for the first pair and up to 600–800 % for the second pair.

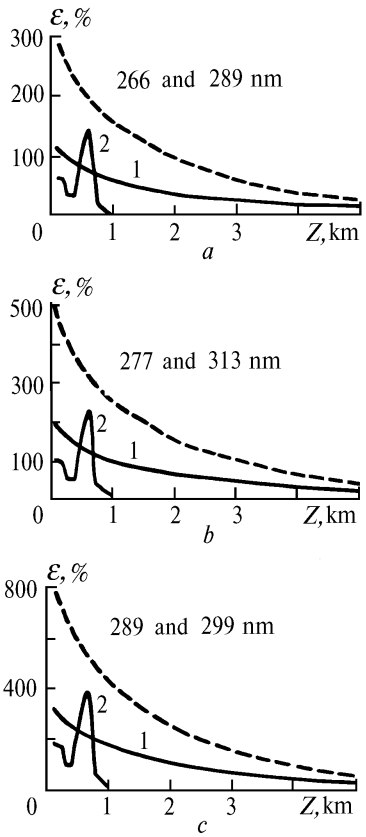

FIG. 3. Relative error in determining the ozone concentration from lidar returns caused by the H_2O *absorption of the UV radiation. Dashed curves show the error due to neglect of the* H_2O *absorption.*

The error decreases rapidly with altitude and at an altitude of ~ 5 km equals to 25 % and 50 % for the first and third pairs, respectively. It should be emphasized once again that the error was calculated for statistical (model) profiles of the H_2O and O_3 concentrations for the mid–latitudes in summer.[40] As mentioned above, the maximum error may be much larger in some cases.

An account of H_2O based on the model data results in a decrease of the error ε (curve *1*), but due to possible deviation of the real profile of H_2O from the model profile by 30 % (see Fig. 1*b*), it is still remaining very large and only at an altitude of 5 km ε decreases down to ~ 10 % for the first pair. The assumption that the H_2O concentration dublicates the model profile, whereas the real profile of H_2O has an inversion shown in Fig. 1*b*, may introduce the error ε shown by curve *2* in Fig. 3.

The error ε caused by model account of optical characteristics of aerosol is shown in Fig. 4. The error was calculated on the basis of the aerosol optical model.[38] The variations δ_{β_a} and δ_{α_a} were borrowed from Ref. 48 and were

equal to 70% while $\delta_{\beta_m} = \delta_{\alpha_m} = 5\%$. The variations δ_{q_α} and δ_{q_β} were taken to be 10%. The effect of spectral behaviour of the aerosol coefficients of backscattering β^a and extinction α^a on $\sigma_{\alpha_{res}}$ is of definite interest. The spectral index q_β according to the data reported in Ref. 7 can vary from 0.5 to 2.0 whereas q_α – from 0.12 to 2.3. According to the data reported in Ref. 31, the value $q_\alpha \in [-1, 3]$. In our calculations let us set $q_\beta = q_\alpha = q$ varying in the range from –1 to 3. The ranges of error variations for all the pairs are shown by dashed lines in Fig. 4. Upper dashed curve corresponds to $q = -1$, the lower one – to $q = 3$, and solid curve – to $q = 1$. The error ε in the ground layer is shown to be maximum and equal to 45 % for $q = -1$ (for the first pair), and for the third pair it is ~ 150 %. The value of ε decreases rapidly with altitude.

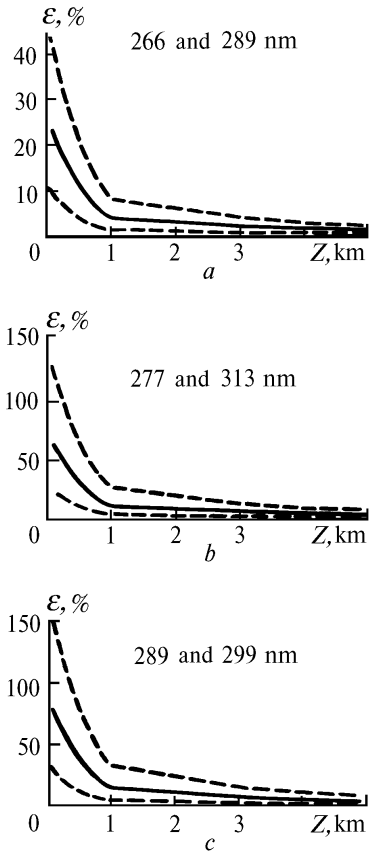

FIG. 4. Relative error in determining the ozone concentration caused by variations in the optical properties of atmospheric aerosol. Dashed curves show maximum and minimum errors.

Let us finally make the main conclusions.

First, the 266 and 289 nm pair is the least sensitive to variations in the atmospheric optical properties among the three pairs. According to the data of the other authors (see, for example, Refs. 14 and 15), it is most suitable for the atmospheric boundary layer.

Second, for successful interpretation of lidar ozone data obtained in the lower troposphere ($H \le 5$ km) the concentration of water vapour must be measured simultaneously. An attempt of using the H_2O model profile failed to correct the systematic error in determining ρ_{O_3}.

Third, correction of lidar return signals for the contribution of aerosol using the model data allows one to decrease the error ε for the first pair of wavelengths down to 5% at altitudes above 2.5 km. At altitudes up to 1 km the error can exceed 10–20%. For the second and third pairs the value of ε is much larger. To reduce it one must carry out simultaneous sounding of atmospheric aerosol.

Fourth, in ozone sounding near industrial areas the measurement of the profiles of SO and NO_2 concentrations is required simultaneously with that of H_2O, at least in the lower 2–km layer.

REFERENCES

1. S. Zaromb, J.F. Avelanet, J. Kiwala, and B.M. Radimer, Laser **3**, No. 1, 21–23 (1971).
2. K. Asai and T. Igarashi, in: Abstracts of Reports at the International Conference on Laser Radar Studies, Sendai (1974), pp. 101–102.
3. I.V. Samokhvalov, A.V. Sosnin, and G.S. Khmel'nitskii, in: *Abstracts of Reports at the All–Union Symposium on Radio–Physical Investigations of the Atmosphere*, Leningrad (1977), pp. 78–82.
4. O.K. Kostko, N.D. Smirnov, and V.V. Fadeev, Kvant. Elektron. **3**, No. 11, 2387–2393 (1976).
5. O.K. Kostko and N.D. Smirnov, in: *Proceeding of the Central Aerological Observatory*, No. 138, 32–47 (1979).
6. O.K. Kostko and N.D. Smirnov, in: *Proceedings of the Sixth All–Union Symposium on Laser and Acoustic Sounding of the Atmosphere*, Tomsk (1980), pp. 199–204.
7. E.D. Hinkley, ed., *Laser Monitoring of the Atmosphere* (Springer Verlag, New York, 1976).
8. R. Gudi, *Atmospheric Radiation* [Russian translation] (Mir, Moscow, 1966), 522 pp.
9. V.P. Gusarov, O.K. Kostko, A.P. Prokhorov, and N.D. Smirnov, in: *Proceedings of the Sixth All–Union Symposium on Laser and Acoustic Sounding of the Atmosphere*, Tomsk (1980), Part I, pp. 222–224.
10. A.J. Gibson and L. Thomas, Nature **256**, 561–563 (1975).
11. G. Megie, J.Y. Allain, M.L. Chanin, and J.E. Blamont, Nature **270**, No. 5635, 349–351 (1977).
12. W.B. Grant and R.D. Hake, J. Appl. Phys. **46**, No. 5, 3019–3024 (1975).
13. O. Uchino, M. Maeda, J. Koho, et al., Appl. Phys. Lett. **33**, No. 9, 807–809 (1978).
14. J. Pelon and G. Megie, Nature **299**, 137–139 (1982).
15. G. Megie and J. Pelon, Planet Space Sci. **31**, No. 7, 791–799 (1983).
16. E.V. Browell et al., J. Geophys. Res. **92**, 2112 (1987).
17. N. Sugimoto, Y. Sasano, S. Hayashida–Amano, et al., in: *Abstracts of Reports at the Fourteenth International Laser–Radar Conference*, Innichen–San–Candido (1988), pp. 187–189.
18. W. Carnuth, ibid., pp. 348–351.
19. P. Bisling, W. Lahmann, C. Weitkamp, and W. Michaelis, ibid., pp. 351–353.
20. S. McDermid, ibid, pp. 388–391.
21. M. Maeda and T. Shibata, ibid., pp. 419–421.
22. A. Papayannis, G. Ancellet, J. Pelon, and G. Megie, ibid., pp. 472–475.
23. M.J.T. Milton, P.T. Woods, B.W. Jolliffe, et al., in: *Abstracts of Reports at the Fifteenth International Laser–Radar Conference*, Tomsk (1990), pp. 164–166.
24. M. Uchiumi, T. Shibata, and M. Maeda, ibid., pp. 264–267.
25. S. Ismail and E.V. Browell, ibid., pp. 300–303.

26. I.G. Shurygin, N.S. Belokrinitskii, V.M. Lagutin, and V.N. Sobolev, Atm. Opt. **3**, No. 10, 965–968 (1990).
27. A.V. El'nikov, V.V. Zuev, V.N. Marichev, and S.I. Tsaregorotsev, Atm. Opt. **2**, No. 9, 841–842 (1989).
28. J. Bosenberg, W. Curnuth, M.J.T. Milton, et al., *TESLAS: Tropospheric Environmenttul Studies by Laser Sounding. EUROTRAC Subproject Proposal.* Annual Report (1991), Part 7.
29. Kh. Okabe, *Fotochemistry of Small Molecules* [Russian translation] (Mir, Moscow, 1981), 500 pp.
30. U. Platt and D. Perner, J. Geophys. Res. **C85**, No. 12, 7453–7458 (1980).
31. O.K. Kostko, in: *Proceedings of the Sixth All–Union Symposium on Laser and Acoustic Sounding of the Atmosphere*, Tomsk (1980), pp. 205–208.
32. V.N. Marichev, A.A. Mitsel', and I.I. Ippolitov, in: *Spectroscopic Methods of Atmospheric Sounding* (Nauka, Novosibirsk, 1985), pp. 44–57.
33. B.M. Klimkin and V.N. Fedorichshev, Atm. Opt. **2**, No. 2, 174–175 (1989).
34. B.M. Klimkin, S.F. Luk'yanenko, I.N. Potapkin, and V.N. Fedorichshev, Atm. Opt. **2**, No. 3, 258–259 (1989).
35. S.F. Luk'yanenko, T.I. Novakovskaya, and I.N. Potapkin, Atm. Opt. **2**, No. 7, 579–582 (1989).
36. S.E. Karmazin, V.M. Klimkin, S.F. Luk'yanenko, et al., in: *Abstracts of Reports at the Fifteenth International Laser–Radar Conference*, Tomsk (1990), 184 pp.
37. S.F. Luk'yanenko, T.I. Novakovskaya, and I.N. Potapkin, Atm. Opt. **3**, No. 11, 1080–1082 (1990).
38. G.M. Krekov and R.F. Rakhimov, *Optical Models of the Atmospheric Aerosol* (Tomsk Affiliate of the Siberian Branch of the Academy of Sciences of the USSR, Tomsk, 1986), 294 pp.
39. V.E. Zuev, *Propagation of Vizible and IR Waves Through the Atmosphere* (Tomsk Affiliate of the Siberian Branch of the Academy of Sciences of the USSR, Tomsk, 1986), 294 pp.
40. I.I. Ippolitov, V.S. Komarov, and A.A. Mitsel', in: *Spectroscopic Methods of Sounding of the Atmosphere* (Nauka, Novosibirsk, 1985), pp. 4–44.
41. V.E. Zuev, ed., *Laser Sounding of the Troposphere and Underlying Surface* (Nauka, Novosibirsk, 1987), 262 pp.
42. H.J. Kolsch, et al., in: *Abstracts of Reports at the Fourteenth International Laser–Radar Conference*, Innichen–San–Candido (1988), pp. 484–487.
43. G.P. Anderson, S.A. Clough, F.X. Kneizus, et al., *AFGL Atmospheric Constituent Profiles* (0–120 km), Report AFGL–TR–86–0110, Environ. Res. Papers No. 954, Hanscom, 1986.
44. V.E. Zuev and V.S. Komarov, *Statistical Models of Temperature and Gaseous Components of the Atmosphere* (Gidrometeoizdat, Leningrad, 1986), 264 pp.
45. P.I. Surkin, V.G. Serzhantov, and V.A. Tvorogov, *Atmospheric Ozone* (Gigrometeoizdat, Moscow, 1990), 120 pp.
46. O. Thomsen, P. Bisling, C. Weitkamp, and W. Michaelis, in: *Abstracts of Reports at the Fifteenth International Laser–Radar Conference*, Tomsk (1990), Vol. 2, pp. 180–183.
47. V.M. Zakharov, ed., *Laser Application to the Determination of the Atmospheric Composition* (Gidrometeoizdat, Leningrad, 1983), 215 pp.
48. V.E. Zuev and G.M. Krekov, *Optical Models of the Atmosphere* (Gidrometeoizdat, Leningrad, 1986), 256 pp.